SOLID PROPELLANT KINETICS. IV. MEASUREMENT OF KINETIC PARAMETERS IN THE OPPOSED FLOW SOLID PROPELLANT DIFFUSION FLAMES

S. J. Wiersma, et al

Stanford Research Institute

Prepared for:

Office of Naval Research

20 December 1973

UNCLASSIFIED

SECURITY CLASSIFICATION OF THIS PAGE (When Data Entered)

REPORT DOCUMENTATION PAGE		READ INSTRUCTIONS BEFORE COMPLETING FORM
1. REPORT NUMBER	2. GOVT ACCESSION NO.	3. RECIPIENT'S CATALOG NUMBER AD773 117
4. TITLE (and Subtitle) SOLID PROPELLANT KINETICS IV. MEASUREMENT OF KINETIC PARAMETERS IN THE OPPOSED FLOW SOLID PROPELLANT DIFFUSION FLAMES		5. TYPE OF REPORT & PERIOD COVERED INTERIM REPORT
		6. PERFORMING ORG. REPORT NUMBER PYU-8378
7. AUTHOR(s) S. J. WIERSMA and H. WISE		8. CONTRACT OR GRANT NUMBER(s) N00014-70-C-0155 Modification No. P0004
9. PERFORMING ORGANIZATION NAME AND ADDRESS STANFORD RESEARCH INSTITUTE 333 Ravenswood Avenue, Menlo Park, CA 94025		10. PROGRAM ELEMENT, PROJECT, TASK AREA & WORK UNIT NUMBERS Project NR 092-507
11. CONTROLLING OFFICE NAME AND ADDRESS Office of Naval Research, Code 473 Power Branch, Washington, D.C.		12. REPORT DATE Dec. 20, 1973 / 13. NO. OF PAGES 38
		15. SECURITY CLASS. (of this report) UNCLASSIFIED
14. MONITORING AGENCY NAME & ADDRESS (if diff. from Controlling Office) Defense Contract Administration Services Region - San Francisco 866 Malcolm Road, Burlingame, CA 94010		15a. DECLASSIFICATION/DOWNGRADING SCHEDULE

16. DISTRIBUTION STATEMENT (of this report)

Distribution of this document is unlimited.

17. DISTRIBUTION STATEMENT (of the abstract entered in Block 20, if different from report)

18. SUPPLEMENTARY NOTES

19. KEY WORDS (Continue on reverse side if necessary and identify by block number)

20. ABSTRACT (Continue on reverse side if necessary and identify by block number)

To examine the gas-kinetics parameters pertinent to the flame reactions of ammonium perchlorate (AP) based propellants we have employed the heterogeneous opposed flow diffusion flame. In this combustion system a diffusion flame is formed in the stagnation region between a gaseous stream of fuel and an opposing stream of oxidizer originating at the solid surface of AP. With increasing fuel flux the steady-state mass flux of AP reaches a value at which the kinetics of reaction limit the consumption of reactants. This limiting condition provides

37

DD FORM 1 JAN 73 1473

EDITION OF 1 NOV 65 IS OBSOLETE

UNCLASSIFIED

SECURITY CLASSIFICATION OF THIS PAGE (When Data Entered)

19. KEY WORDS (Continued)

20 ABSTRACT (Continued)

(Continued from Block 20)

information on the gas phase kinetic parameters of the combustion system. Both the composition of the solid oxidizer and the gaseous fuel were varied in the experimental studies. The effects of different catalysts and solid fuels were examined on the burning rate characteristics of the solid phase. A number of gaseous hydrocarbon fuels were used. Based on the results kinetic expressions are derived for the overall combustion progress in the diffusion flame of solid propellants based on AP.

CONTENTS

ILLUSTRATIONS

TABLES

INTRODUCTION

Current theoretical models[1] of composite solid propellant combustion are based on an analysis of heat transfer from a two-stage flame to the solid surface undergoing sublimation.[1,2] The first stage of the flame is considered to be a thin, premixed reaction zone fed by ammonia and perchloric acid from the decomposition of ammonium perchlorate (AP). In the second stage, the combustion of fuel and oxidant molecules is postulated to occur under conditions controlled by diffusional mass transport and chemical reaction rates. Although such a model does not take into account the heterogeneous reactions occurring near the subsurface of the propellant and at the solid/gas interface,[3,4] especially in the presence of catalysts and fuels, it has been moderately successful in providing a semiquantitative description of the burning characteristics of propellants as a function of such variables as gas pressure and AP particle size. However, to advance and refine the theoretical model further, one needs quantitative information on the kinetics of the gas-phase reactions of the propellant components at flame temperatures.

An experimental approach to this problem is the heterogeneous opposed flow diffusion flame (HOFD) fed by two sources; one a solid oxidizer and the other a gaseous fuel. This technique is based on earlier work done by Potter and coworkers,[5,6] who demonstrated that the extinction of a homogeneous diffusion flame formed between opposing fuel and oxidizer jets, is a measure of the maximum reaction rate attainable. A theoretical analysis[7] of the homogeneous diffusion flame dealt with the relationships between the mass fluxes of fuel and oxidant at extinction and the laminar flame speed in premixed gases. We have extended this work to an evaluation of the kinetic parameters of the combustion system from the extinction conditions ("apparent flame strength").[8]

For the solid propellant system, the HOFD uses the surface of the solid propellant as the source of one of the reactants (A); while the other reactant (B) is a gas emanating from a cylindrical tube located normal to and at some distance from the propellant surface. A flat diffusion flame forms in the intervening space. The steady state regression rate of the solid propellant with increasing mass flux of B is monitored. A limiting condition is reached at which point the mass flux of the solid reactant becomes independent of that of B. At this point, the rate limiting chemical kinetics can no longer consume all the reactant being fed into the combustion zone. In 1961 Friedman[9] made some preliminary measurements of the burning rate of AP onto which a jet of gaseous fuel was impinging. More recently the steady-state linear pyrolysis of several thermoplastic materials was measured with the aid of an opposed jet flame.[10] But in neither case did the data provide information on the flame kinetics because of the limited range of experimental measurements.

EXPERIMENTAL DETAILS

Burning Rate Studies

The HOFD experimental apparatus is depicted in Figure 1. Inside a large glass cylinder, the reaction chamber, a gas jet containing fuel and diluent is allowed to impinge on the surface of a solid propellant composed of ammonium perchlorate (AP) with catalyst and solid fuel additives. The solid is contained in a copper block provided with a closely fitting opening through which the propellant is advanced by a motor-driven mechanical piston. The top surface of the solid is perpendicular to the gas jet. The two units have a common centerline, but the distance between them may be adjusted.

After ignition of the propellant strand by an electrically heated resistance wire, a flame is established in the stagnation region formed by the flow of gaseous fuel and of AP decomposition products. For a given mass flux of gaseous fuel, the steady-state consumption rate of the solid propellant is measured by matching the rate of advance of the propellant strand to its consumption rate, so that the distance between the gaseous fuel outlet and the propellant surface remains constant. Condensation of liquid combustion products on the cool portions of the propellant is obviated by providing the opening in the copper block with a small conical section. (Figure 1). The combustion products are swept away by a carrier stream (N_2) which enters the cylindrical chamber through openings in the support plate located at the bottom of the apparatus.

In a series of measurements it was observed that a distance of 6 mm between the fuel gas outlet and the solid propellant surface result in a flame of high stability and cylindrical shape. At smaller distances the

solid tended to form a conical surface and the flame tends to conform to this shape. At larger distances the flame tended to become less stable.

The propellant strand diameter was 6 mm. The cylindrical delivery tube for the gaseous fuel had a diameter of 25 mm, and was water cooled to prevent preheating. When the diameter of the fuel jet exceeded by a factor of four that of the propellant, the steady-state propellant mass flux for a given fuel gas velocity was found to be independent of the jet size.

A typical experiment consisted of measuring over a range of mass fluxes of gaseous fuel, M_g, the steady-state mass flux of solid propellant, M_s, necessary to feed the diffusion flame. A distance of 6 mm between the outlet of the fuel jet and the solid-propellant surface was constantly maintained with the aid of a cathetometer. The appearance of the diffusion flame is shown in Figure 2. The solid has assumed a slightly convex surface, a condition that does not seem to affect M_s materially. The striations visible in the photograph result from the particulate combustion products of the copper chromite (CC) catalyst passing through the diffusion flame. Their luminous streaks are indicative of the flow pattern prevailing near the flame.

The solid strands were prepared from crystalline AP, oven dried at 120°C, ball-milled, and sieved into size-graded fractions. The particle size of the AP was limited to the range from 61 to 89 microns. Powdered catalyst, or solid fuels, or both, were added to the AP. The powdered mixture was pressed at 30,000 psi into 6.0-mm diameter strands.

Temperature Studies

Surface Temperature:

Chromel-alumel thermocouples, constructed from wires (2 mils in diameter), were used to measure the temperature in the solid strands.

A thermocouple was first mounted in the die in which the strands were pressed. The powdered mixture was then poured around the thermocouple an and pressed in the mandrel illustrated in Figure 3.

The temperature was recorded as the thermocouple bead advanced toward the surface (Figure 4). During a typical measurement the recorded temperature increased smoothly and monotonically up to the phase transition of the AP lattice at 240°C.[11] where a short plateau occurred. This plateau was followed by a rapid temperature rise with a break in the profile at a point where the thermocouple emerged from the surface.

Flame Temperature:

The flame temperature was measured by the conventional sodium line reversal method. The flame was spiked with NaCl by depositing a small amount of the salt on the metal screen closest to the flame through which the gaseous fuel passed. (See Figure 1). The image of a tungsten ribbon filament lamp was focussed on the plane of the axis of the burner. This image was then focussed on the slit of a spectroscope. An iris was placed between the flame and the spectroscope which admitted to the spectroscope only the cone of light originating at the lamp filament. The temperature of the lamp filament used for the measurements was calibrated with an optical pyrometer.

EXPERIMENTAL RESULTS

Steady-State Burning Rate Measurements

Of special interest to our study were the linear regression rates of solid propellant strands during steady-state combustion as a function of: 1) the composition of the solid phase with respect to catalyst and fuel content, and 2) the composition of the gas phase in terms of fuel type and concentration. The effect of catalyst on the steady-state regression rate of the solid phase is shown in Figure 5, with methane, and in Figure 6, with propylene, as a fuel. The mass flux of solid as a function of the mass flux of gaseous fuel in the opposing jet markedly increased by the addition of copper chromite catalyst to the AP strand. Similar effects were observed in the presence of other catalysts as summarized in Figure 7.

The contribution of a solid fuel additive (sucrose octaacetate, SO) to the burning characteristics of AP-strands in the HOFD is shown in Figure 8. Again it is found that an increase in organic fuel concentration in the condensed phase caused a significant increase in the regression rate of the solid at various concentrations of C_3H_6 in the opposed jet. Also the data indicated a finite rate of solid propellant burning in the absence of gaseous fuel in the opposed jet. Other solid fuel additives, such as Delrin polymer and Norit-A carbon were examined (Figure 9). In the presence of both fuel and catalyst additives the regression rate of the solid phase was enhanced still further (Figure 10).

A somewhat different picture emerges from the results obtained for different gas-phase compositions. Typical results for C_3H_6 are to be found in Figure 11 for the case of pure AP, and in Figures 12 and 13 for AP/catalyst as the condensed phase.

Limiting Mass Fluxes

A common characteristic of our studies with the HOFD is the upper limit in the mass flux of solid oxidizer M_s^* exhibited at high mass fluxes of the gaseous fuel component (Figures 5-13). The condition at which the consumption rate of solid oxidizer becomes independent of M_g represents the region in which the reaction kinetics in the flame zone limit the consumption of reactants.[7,8] In exploring the relationship between the limiting mass fluxes of solid oxidizer and gaseous fuel as a function of the inlet composition of the condensed and gaseous phases we define as M_g^* the mass flux of gaseous fuel at which M_s^* is attained. The results for different solid-phase and gas-phase compositions are given in Table 1. These data point to the fact that the value of M_g^* is predominantly a function of the composition of the gaseous fuel fed into the HOFD, and relatively unaffected by the solid-phase composition (Figure 7). On the other hand, for a given gaseous fuel composition, the limiting mass flux of solid M_s^* exhibits variations that reflect the makeup of the condensed phase in terms of catalyst and fuel additives (Figures 5, 6, 8, and 10).

Surface and Flame Temperature Measurements

In the region of steady-state burning the surface-temperature measurements indicate a nearly linear relationship between the mass flux of the solid phase (AP/CC) and the temperature of the regressing solid surface. (Figure 14). Such a linear relationship is maintained over a wide range of gaseous fuel compositions undergoing combustion in the HOFD. Although the number of measurements carried out for different compositions of the solid phase is small, the linear variations of regression rate and surface temperature appears to apply equally well to systems containing a solid phase made up of AP, catalyst, and sucro-octaacetate fuel (SO) (Figure 14). For each of these solid

propellant compositions the curves extrapolate to a value below which steady-state deflagration ceases. For the system 97.1 AP/2.9 CC/C_3H_6 one finds this temperature to be nearly 550^{o}K, while for the system 93.3 AP/1 CC/ 5.7 SO/C_3H_6 the limiting surface temperature is found to be near 280^{o}K.

A comparison of several steady-state surface and flame temperature determinations for different solid propellant systems demonstrates that for a given propellant mass flux the flame temperature decreases as CC-catalyst is added to the solid phase (Table 2). At the same time the corresponding surface temperature increases. These trends are indicative of the contribution of solid-phase reactions that raise the surface temperature because of their exothermicity but lower the flame temperature because of reactant depletion at the solid/gas interface.

DISCUSSION

In examining the experimental results obtained by the HOFD technique we consider first the steady-state burning aspects of the solid propellant/gaseous fuel systems. In many respects these systems exhibit the behavior of diffusion flames established during liquid fuel droplet burning in the presence of a forced convection field.[14,15] The mass flux from the condensed phase was shown to be a function of the transfer function, containing the Reynolds number Re, a term describing the flow properties of the system, and the transfer number B, a term related to the thermodynamic and gas properties of the system:

$$M_s = f\,(Re,B)$$

The transfer function f (B) is given by:

$$f\,(B) = \frac{M_s \cdot d}{\mu}/\sqrt{Re} \qquad (1)$$

where M_s is the mass flux of the condensed phase, d is the diameter of the condensed phase* from which reactant is fed into the diffusion flame, μ is the absolute viscosity of the gas, and Re is the Reynolds number of the gas ($Re = Ud/\nu$, where U is the gas stream velocity and ν is the kinematic viscosity of the gas).

In applying this theory to the steady-state burning rate data we expect the mass flux of solid propellant to be proportional to the square root of the Reynolds number of the gaseous fuel in the opposing jet. We have examined this relationship for the AP/C_3H_6 system (Figure 15). Indeed the rate of gasification of solid material (AP) is proportional to the half-power of the mass flow of gaseous fuel (C_3H_6). Table 3 compares the transfer function f (B) for a number of compositions of the solid

*For the HOFD system d represents the diameter of the propellant strand which during combustion acquires a radius of curvature within 10 percent of this value.

phase. It is found that the addition of CC-catalyst causes a constant relative increase in the value of the transfer function by a factor of 1.65 over that observed in the absence of the catalyst. The magnitude of this increase is independent of the gas-phase composition, which in our study, was varied from 24 to 100 vol% C_3H_6. However the limiting mass flux is reduced in the presence of 100 vol% C_3H_6 from that observed at lower fuel concentrations. This effect appears to be due to the differences in the heat capacity of C_3H_6 as compared to N_2. At the high mass fluxes encountered in the region of limiting mass flux, C_3H_6 becomes a more effective diluent than nitrogen by carrying away heat more readily from the flame region.

On the basis of the theoretical relationship[14,15] we can evaluate the transfer numbers B from the experimental mass transfer rates (Table 3). As evidenced by the data, the values of B (as evaluated from Figure 10 in Reference 15) are nearly proportional to the fuel concentration in the gas stream at the source, for each of the solid oxidizer systems examined (AP and AP/CC). Such a dependency is to be expected on the basis of Eq. (1) and the definition of B:

$$B = \frac{Y_{go}}{i}\frac{Q}{L} + \frac{C(T_{go}-T_s)}{L} \qquad (2)$$

where Y_{go} represents the mass fraction of gaseous fuel at the source, i the stoichiometric mixture ratio (wt basis); Q, the heat of combustion, L the net heat of sublimation, C the specific heat, T_s the surface temperature, and T_{go} the gas stream temperature at the source.

In the absence and presence of additives the pronounced effect of condensed-phase reactions on the AP regression rate makes difficult an estimate of the net heat of sublimation of reactants from the solid surface. Obviously the endothermic heat of sublimation of AP will be modified by the contribution of exothermic reactions in the condensed

phase. However from each of the B-values listed in Table 3 we can compute with the aid of Equation (2) the effective heat of sublimation L, the net heat required to transfer material across the solid-gas interface. In this calculation we used a value of i = 2.5 and Q = 490 kcal/mole, corresponding to the stoichiometry and heat of combustion for propylene. The values of L were found to be 140 cal/g for the AP and 50 cal/g for the 97.1 AP/2.9 CC-catalyst system, as compared to the latent heat of sublimation of AP (490 cal/g).[16] Again we are led to conclude that the differences observed are attributable to exothermic condensed-phase reactions during the burning-rate experiments with AP, and with AP catalyst.

The contribution of solid-phase reactions is further emphasized by the HOFD data obtained in the presence of different catalysts added to AP (Figure 7). The slope of the lines, relating the mass flux of solid to that of gaseous fuel, increases in the sequence $Fe_2O_3 < CuO < Cr_2O_3$. This sequence is identical to that expected on the basis of previous experimental studies of the heat-release kinetics of AP in the presence of these catalysts.[3] Also the HOFD data indicate that on a weight basis the regression rate of AP is more greatly enhanced by CR_2O_3 than by CC. However in the presence of a solid fuel additive to the AP phase the relative effectiveness of the two catalysts is reversed (CC > Cr_2O_3), an indication that CC plays the role of a dual-function catalyst by promoting not only the decomposition of AP but also the oxidation of fuel.[4]

It should be noted that the results for the combustion of AP-spheres in a propane gas stream[17] lend themselves to the same theoretical analysis. In Figure 15 we have indicated by a dashed line the data for AP/propane. The derived value of the transfer number B is listed in Table 3, together with the net heat of sublimation L calculated on the basis of this value. Good agreement is noted between the values of L obtained from the experiment with C_3H_6 and C_3H_8.

Next we turn to an examination of the limiting combustion conditions exhibited by the HOFD of the various systems under study. The steady-state burning data are interpretable in terms of an infinitely thin reaction zone, due to the controlling influence of physical processes involving mass and heat transport. However the "extinction condition", i.e., the upper limit in the regression rate of the condensed phase, is governed by limitations imposed by the chemical gas-phase kinetics of the fuel/oxidizer system. This conclusion, reached in earlier studies of droplet burning with forced convection,[12,13] applies also to our HOFD experiments. On the basis of the analysis of diffusion flame extinction[14] we can obtain valuable information on the kinetic reaction parameters from the limiting mass fluxes measured in our studies. Such calculations result in the following rate expression for an assumed second-order gas-phase reaction between propylene and the oxidizer species emanating from the solid surface composed of AP or AP/CC:

$$k = 3 \times 10^{12} \exp(-30000/RT)(\text{mol/cc})^{-1}\text{sec}^{-1}.$$

Evaluation of the net sublimation energy of the condensed phase (Table 3) in combination with the measured mass flux rates leads to an estimate of the temperature gradients established at the solid/gas interface. At the limiting mass flux condition the results shown in Table 4 obtain. Although the surface temperature gradient is somewhat lower for AP/CC than for AP, the regression rates differ in the opposite direction by a factor of nearly two. Again we see the contribution of the exothermic condensed phase reactions that consume reactant, thereby increasing the surface temperature and lowering the temperature gradient. The experimental temperature gradients at the solid/gas interface measured by the thermocouple technique are in reasonable agreement with theoretical calculations.

The boundary layer approximation[14,15] has been used in the interpretation of our experimental HOFD data. However it is recognized that the experimental conditions encountered in the HOFD are inadequately approximated by a basic assumption of boundary layer theory, namely that the variation in the mass flux vector is greater perpendicularly than along the boundary. Work in progress[18] employs a fluid-dynamic model more closely akin to the stagnation point flow of the HOFD. This model is expected to yield a more accurate description of the problem and a more precise interpretation of the kinetic processes in the HOFD and their application to different solid-propellant combustion models.

REFERENCES

1. M. Summerfield et al., Progress in Astronautics and Rocket Series, Academic Press, New York, 1960, Vol. I, p. 14.

2. J. A. Steinz, P. L. Lang, and M. Summerfield, AIAA Preprint 68-658.

3. S. H. Inami, W. A. Rosser, and H. Wise, Combustion and Flame 12, 41 (1968).

4. S. H. Inami, Y. Rajapakse, R. Shaw, and H. Wise, Combustion and Flame 17, 189 (1971).

5. A. E. Potter and J. N. Butler, J. Am. Rocket Soc. 29, 154 (1959).

6. A. E. Potter, S. Heimel, and J. N. Butler, Eighth Symposium on Combustion, Williams and Wilkins Co., Baltimore, Md., 1962, Paper No. 108.

7. D. B. Spalding, J. Am. Rocket Soc. 31, 763 (1961); Int. J. Heat Mass Transfer 2, 283 (1961).

8. C. M. Ablow and H. Wise, "A Chemical Kinetics Model for the Opposed-Flow Diffusion Flame," Combination and Flame (in press).

9. R. Friedman, quoted in Ref. 7.

10. R. F. McAlevy, S. Y. Lee, and W. H. Smith, AIAA J. 6, 1137 (1968).

11. L. L. Bircumshaw and B. H. Newman, Proc. Roy. Soc., (London) A227, 115 (1965).

12. G. Agoston, H. Wise, and W. A. Rosser, Sixth Internat. Symposium on Combustion, Reinhold Publishing Co., New York (1956) Paper No. 93.

13. D. B. Spalding, Fourth Internat. Symposium on Combustion, Williams & Wilkins, New York (1953), p. 847.

14. D. B. Spalding, Fuel 33, 255 (1954).

15. D. B. Spalding, Proc. Roy. Soc. (London) A221, 78 (1954).

16. S. H. Inami, W. A. Rosser, and H. Wise, J. Phys. Chem. 67, 1077 (1963).

17. L. Nadaud, ONERA, Tech. Rep. No. 298 (1965).

18. C. M. Ablow and H. Wise (to be published).

Table 1

CRITICAL MASS FLUX DATA FOR HOFD

Solid Phase (wt%)			Gas Phase** (vol%)	M_s^*	M_g^*	M_s^*/M_g^*
AP	Catalyst*	Fuel		$(g \cdot cm^{-2} sec^{-1}) \times 10^2$		
100	0	0	24 CH_4	2.7	1.2	2.2
97.1	2.9 CC	0		4.1	1.2	3.4
95.2	4.8 CC	0		4.8	1.1	4.4
100	0	0	24 C_3H_6	3.1	1.5	2.1
97.1	2.9 CC	0		5.2	1.5	3.5
95.2	4.8 CC	0		6.9	1.5	4.6
100	0	0	50 C_3H_6	3.9	1.0	3.9
97.1	2.9 CC	0		7.6	1.1	6.5
95.2	4.8 CC	0		9.8	1.2	8.2
100	0	0	100 C_3H_6	3.6	0.8	4.5
97.1	2.9 CC	0		6.4	0.7	9.1
95.2	4.8 CC	0		8.6	0.7	12.3
99.0	1.0 Cr_2O_3	0	24 C_3H_6	5.2	1.5	3.5
99.0	1.0 CuO	0		4.5	1.5	3.0
97.1	2.9 Cr_2O_3	0		9.7	1.5	6.4
97.1	2.9 Fe_2O_3	0		3.3	1.4	2.4
97.1	0	2.9 SO	24 C_3H_6	7.1	1.4	5.1
96.1	1.0 CC	2.9 SO		9.1	1.3	7.0
96.1	1.0 Cr_2O_3	2.9 SO		7.2	1.5	4.8
96.1	1.0 CuO	2.9 SO		8.4	1.5	5.6
94.3	0	5.7 SO	24 C_3H_6	8.2	1.3	6.3
93.3	1.0 CC	5.7 SO		10.5	1.3	8.1
93.3	1.0 Cr_2O_3	5.7 SO		9.6	1.5	6.4
93.3	1.0 CuO	5.7 SO		11.4	1.5	7.6
90.0	0	10.0 SO	24 C_3H_6	16.0	1.0	16.0
89.0	1.0 CC	10.0 SO		21.0	1.1	19.1
89.0	1.0 Cr_2O_3	10.0 SO		17.8	1.4	12.7
89.0	1.0 CuO	10.0 SO		20.1	1.4	14.4
97.1	0	2.9 Delrin	24 C_3H_6	6.1	1.5	4.1
96.1	1.0 CC	2.9 Delrin		8.9	1.5	5.9
97.1	0	2.9 Norit A	24 C_3H_6	9.0	1.4	6.4

*CC = copper chromite catalyst; SO = sucrose octaacetate

**Diluent gas: N_2

Table 2

SURFACE AND FLAME TEMPERATURES OF HOFD

Gas (vol %)		Solid (wt %)			$M_s \times 10^2$	T_s	T_f
C_3H_6	N_2	AP	Catalyst*	Fuel**	($g \cdot cm^{-2} \cdot sec^{-1}$)	(K)	(K)
24	76	100	0	0	3.1	700	1745
		97.1	2.9	0	3.1	770	1525
24	76	97.1	2.9	0	5.2	850	1915
		95.2	4.8	0	5.2	913	1645
24	76	94.3	0	5.7	8.0	[illegible]	1905
		93.3	1.0	5.7	8.0	855	1875

*Catalyst: copper chromite (CC)

**Fuel: sucrose-octaacetate (SO)

Table 3

EVALUATION OF TRANSFER NUMBER

Solid	Gas		Transfer Function	L	Transfer Number
AP/CC (wt %)	Fuel	Concentration (wt %)	f(B)	cal/g	B
100/0	C_3H_6	0.32	5.5	150	8
	C_3H_6	0.60	8.4	130	18
	C_3H_6	1.00	10.0	160	30
97.1/12.9	C_3H_6	0.32	9.1	48	25
	C_3H_6	0.60	13.2	48	50
	C_3H_6	1.00	17.5	53	90
100/0*	C_3H_8	1.00	9.4	130	25

*Based on data obtained by Nadaud (ONERA, Tech. Rep. 298 (1965)

Table 4

SURFACE TEMPERATURE GRADIENTS

Gas		Solid		Limiting Mass Fluxes		Surface Temp.	Surface Temp. Gradient	
(vol %)		(wt %)		($g \cdot cm^{-2} \cdot sec^{-1}$)		(K)	($K \cdot cm^{-1}$)	
C_3H_6	N_2	AP	CC	M_s^*	M_g^*	T_s	$\left(\frac{dT}{dx}\right)_{calc}$	$\left(\frac{dT}{dx}\right)_{expt}$
24	76	100	0	0.031	0.015	700	4.6×10^4	2.0×10^4
24	76	97.1	2.9	0.052	0.015	850	2.6×10^4	1.6×10^4

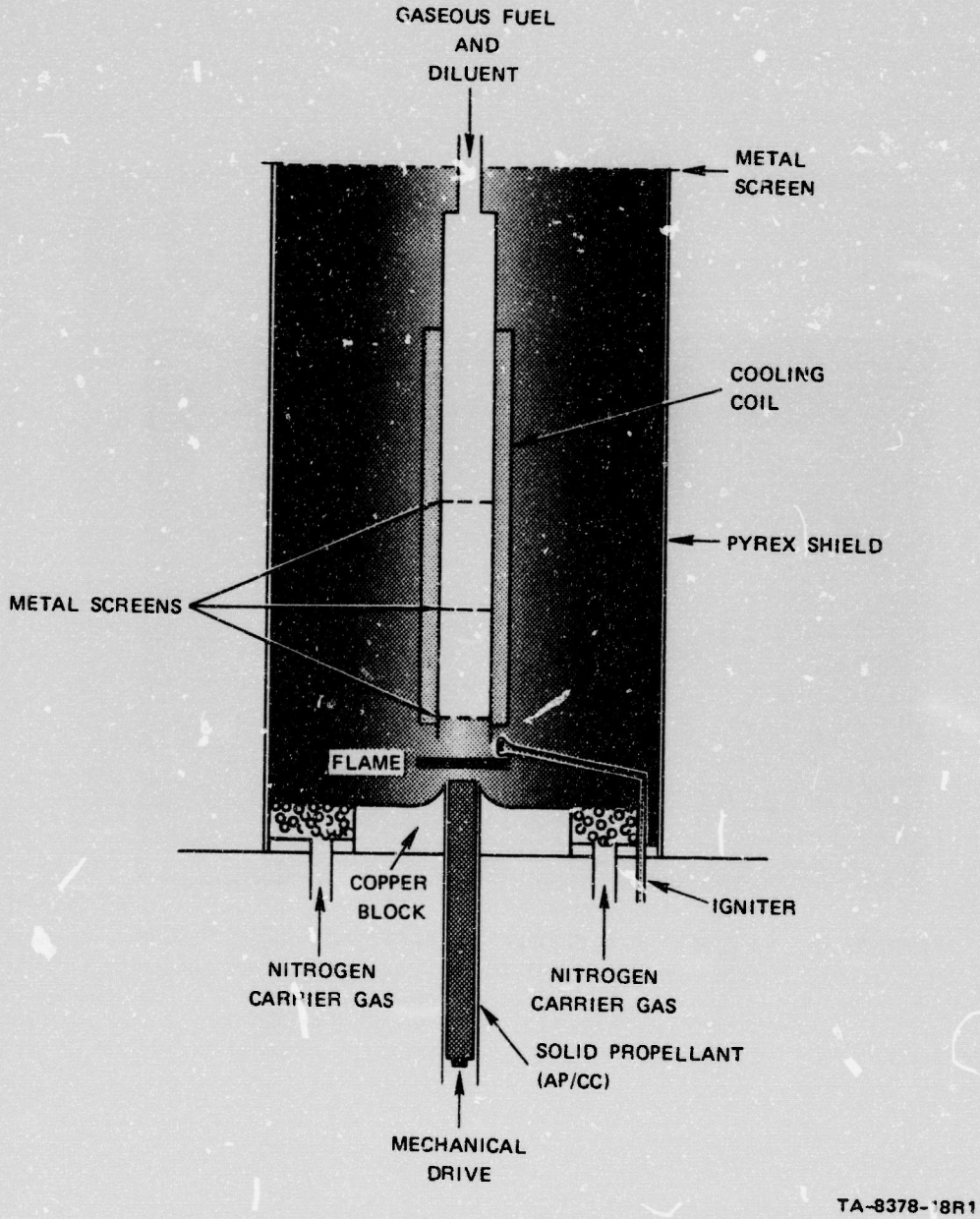

FIGURE 1 APPARATUS FOR HETEROGENOUS OPPOSED FLOW DIFFUSION FLAME

Preceding page blank

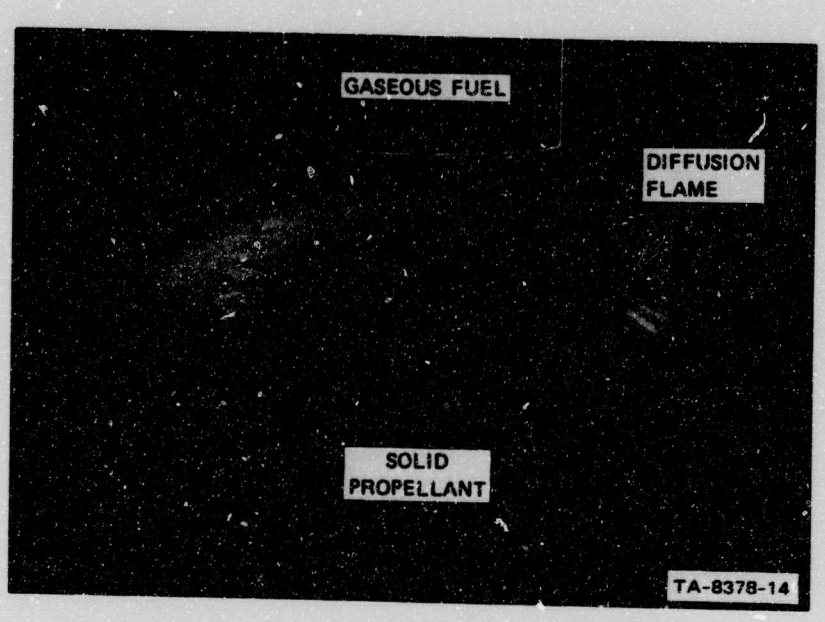

FIGURE 2 HETEROGENEOUS OPPOSED FLOW DIFFUSION FLAME
(Solid Propellant: AP/3CC; Fuel: CH_4 [24% vol.])

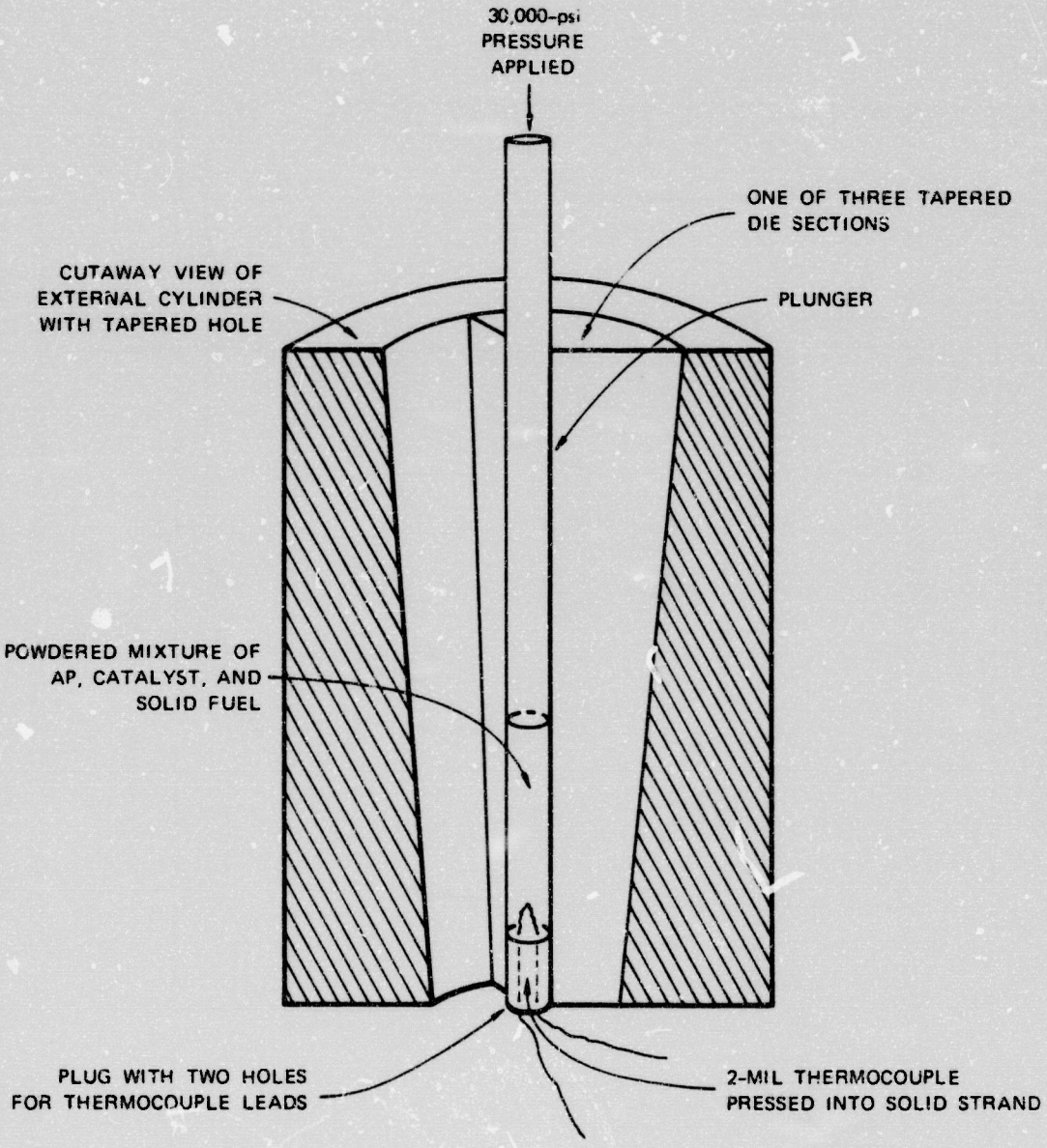

FIGURE 3 DIAGRAM OF MANDREL FOR PREPARATION OF SOLID STRANDS

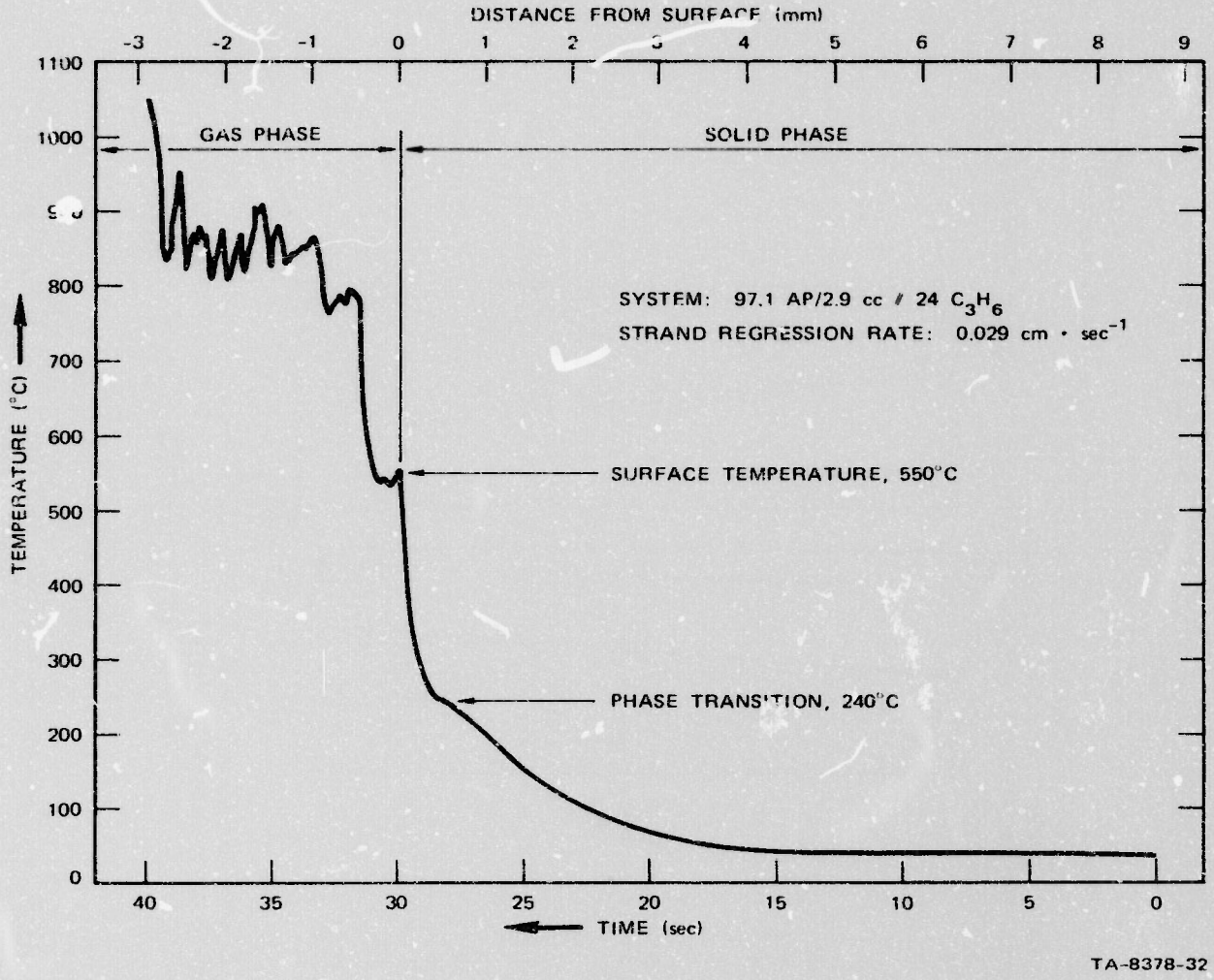

FIGURE 4 TYPICAL TEMPERATURE HISTORY OF CONDENSED PHASE IN HOFD

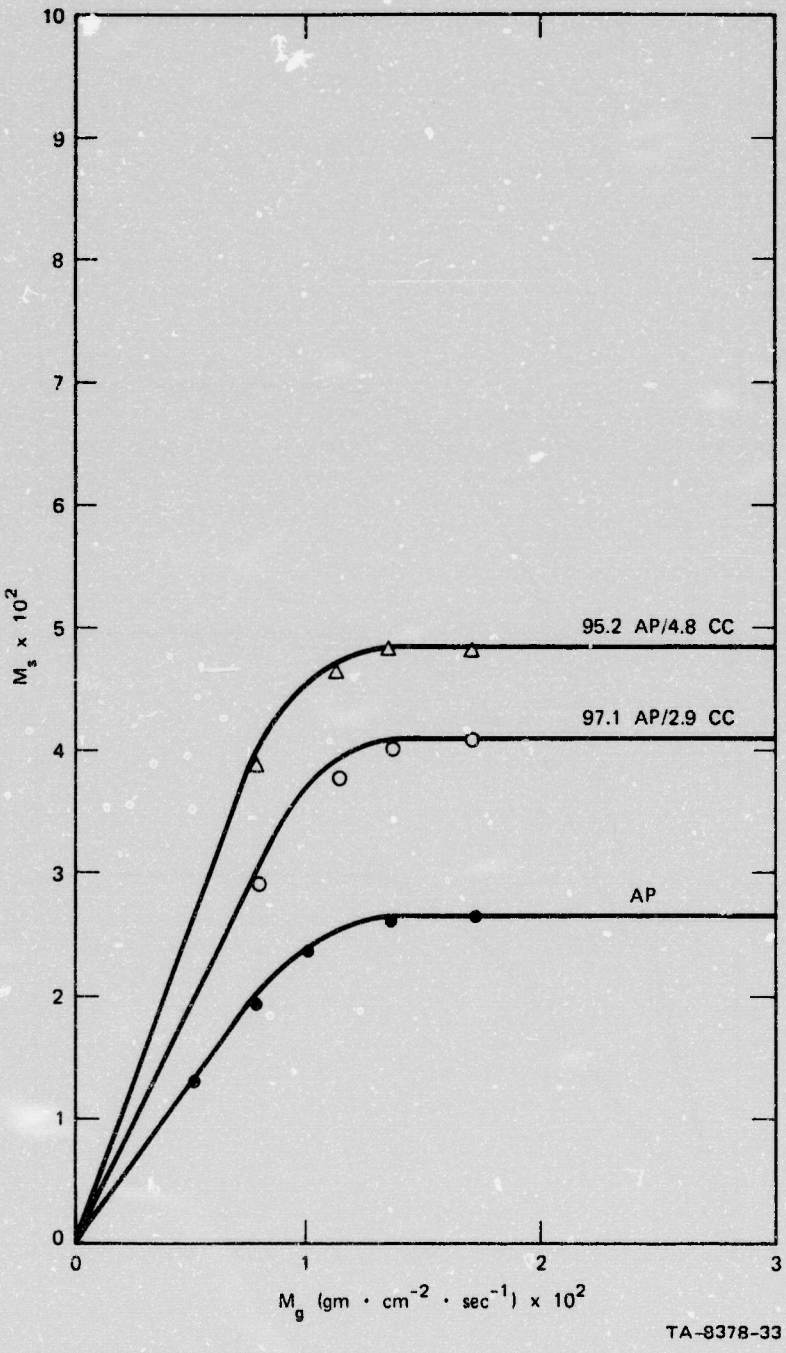

FIGURE 5 HOFD DATA FOR SYSTEM: AP/CH_4 WITH AND WITHOUT CATALYST (CC) (AP = $NH_4C\ell O_4$; CC = COPPER CHROMITE; GAS: 24 VOL% CH_4)

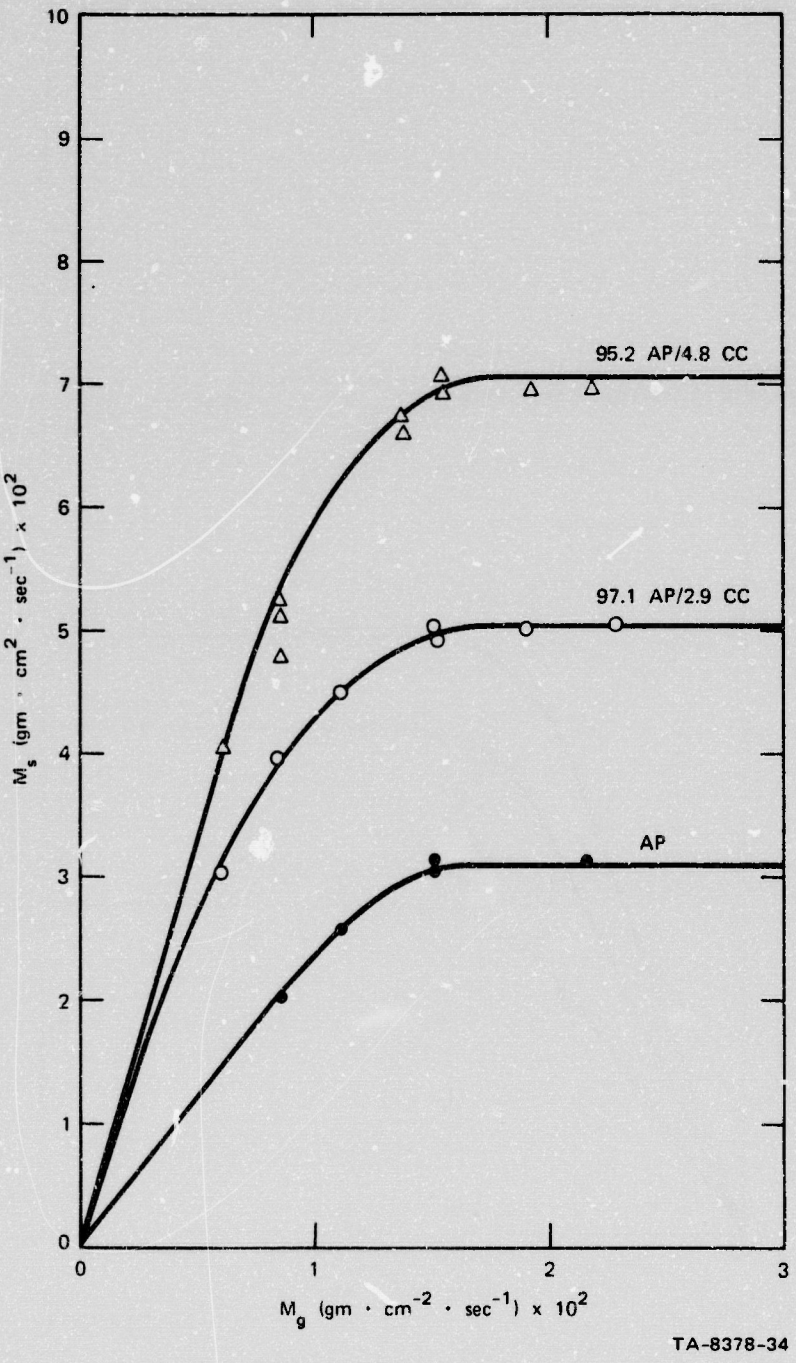

FIGURE 6 HOFD DATA FOR SYSTEM: AP/C_3H_6 WITH AND WITHOUT CATALYST (CC) (AP = NH_4ClO_4; CC = COPPER CHROMITE; GAS: 24 VOL% C_3H_6)

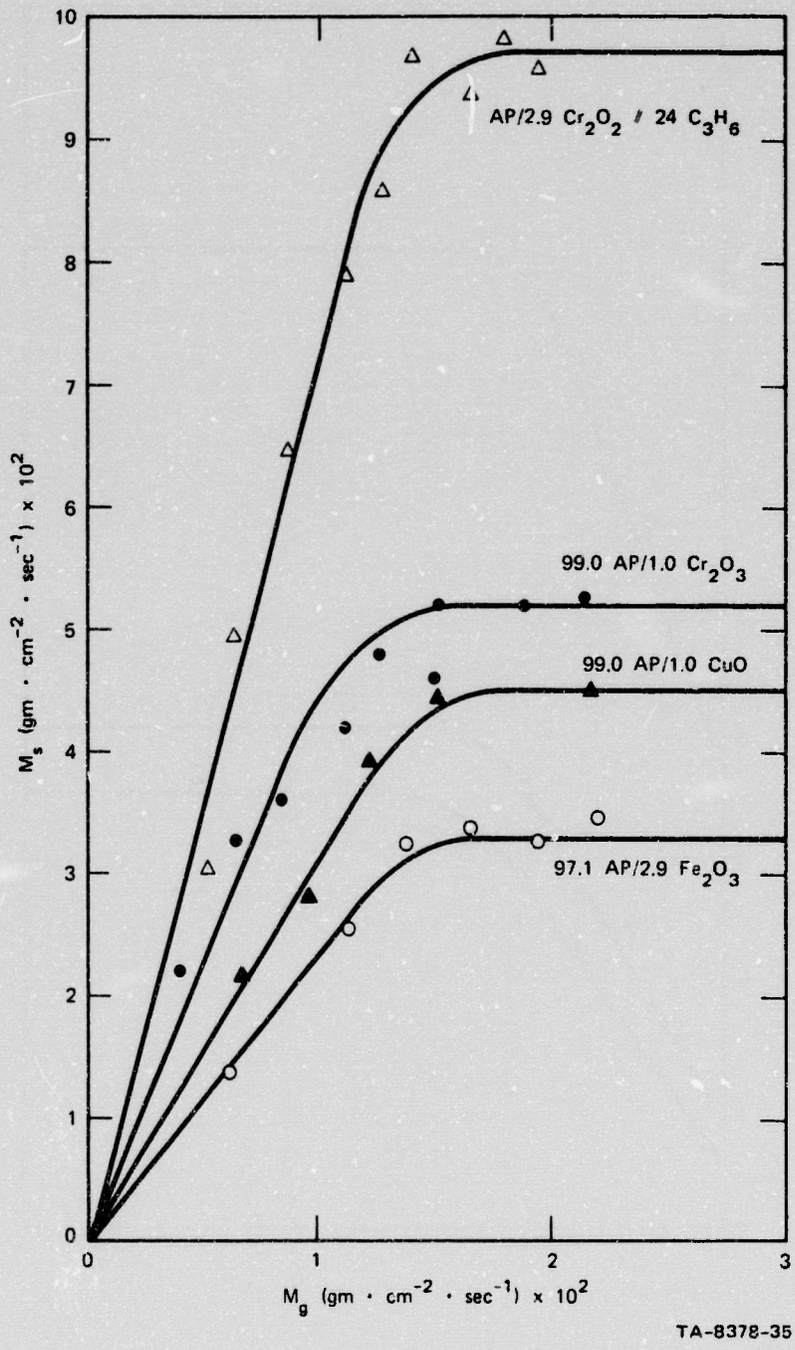

FIGURE 7 EFFECT OF DIFFERENT CATALYSTS ON BURNING CHARACTERISTICS OF HOFD (SOLID: AP/CATALYST; GAS: 24 VOL% C_3H_6)

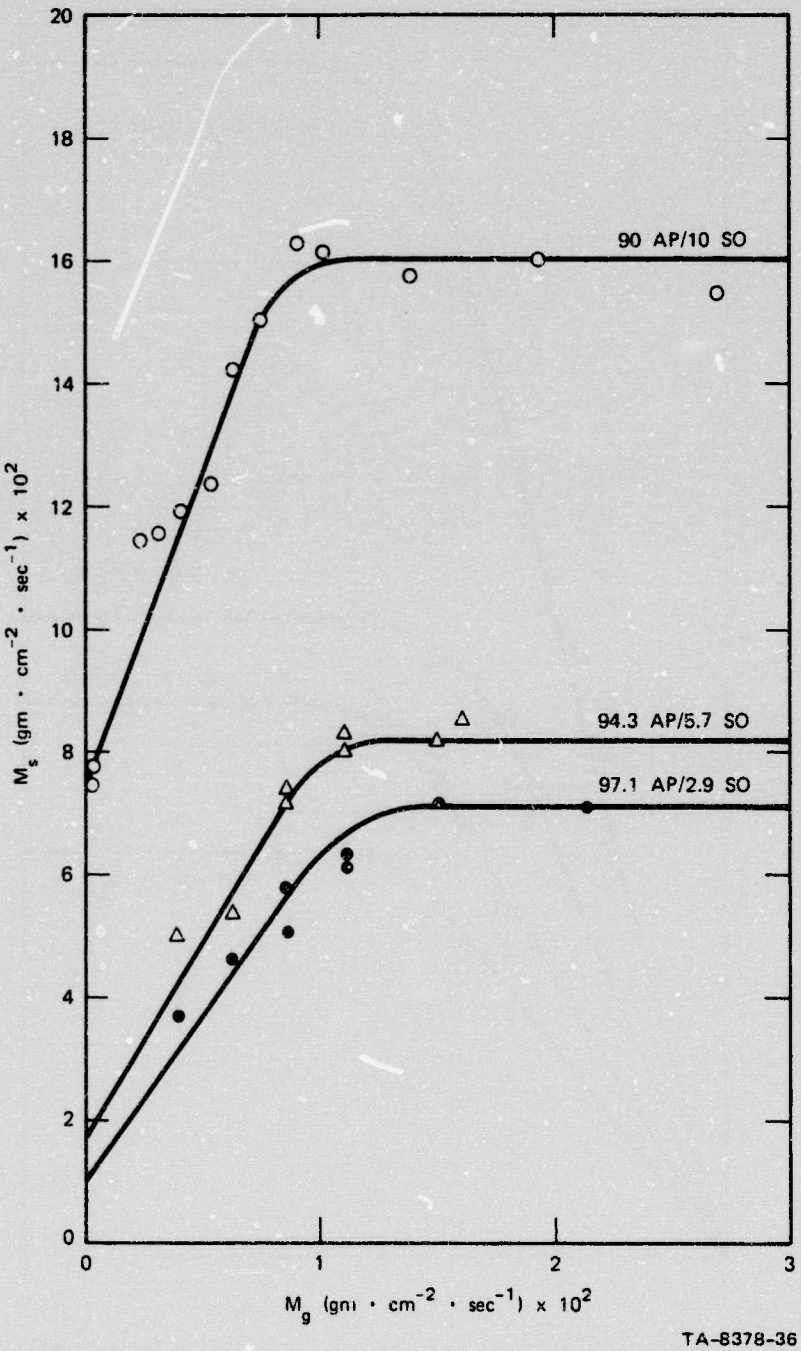

FIGURE 8 CONTRIBUTION OF SOLID FUEL TO BURNING CHARACTERISTICS OF HOFD [SOLID: AP/SUCROSE OCTAACETATE (SO); GAS: 24 VOL% C_3H_6]

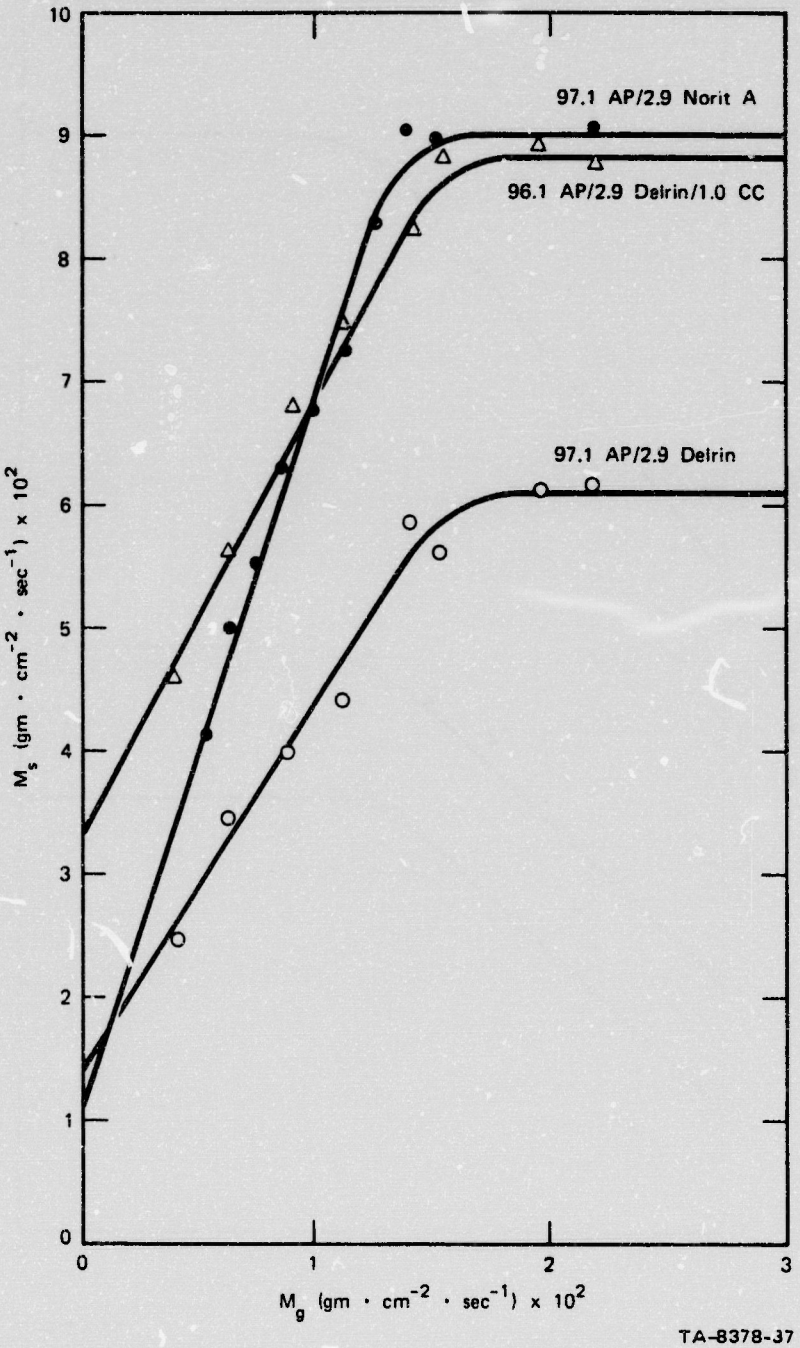

FIGURE 9 EFFECT OF DIFFERENT FUEL ADDITIVES ON BURNING CHARACTERISTICS OF HOFD (GAS: 24 VOL% C_3H_6)

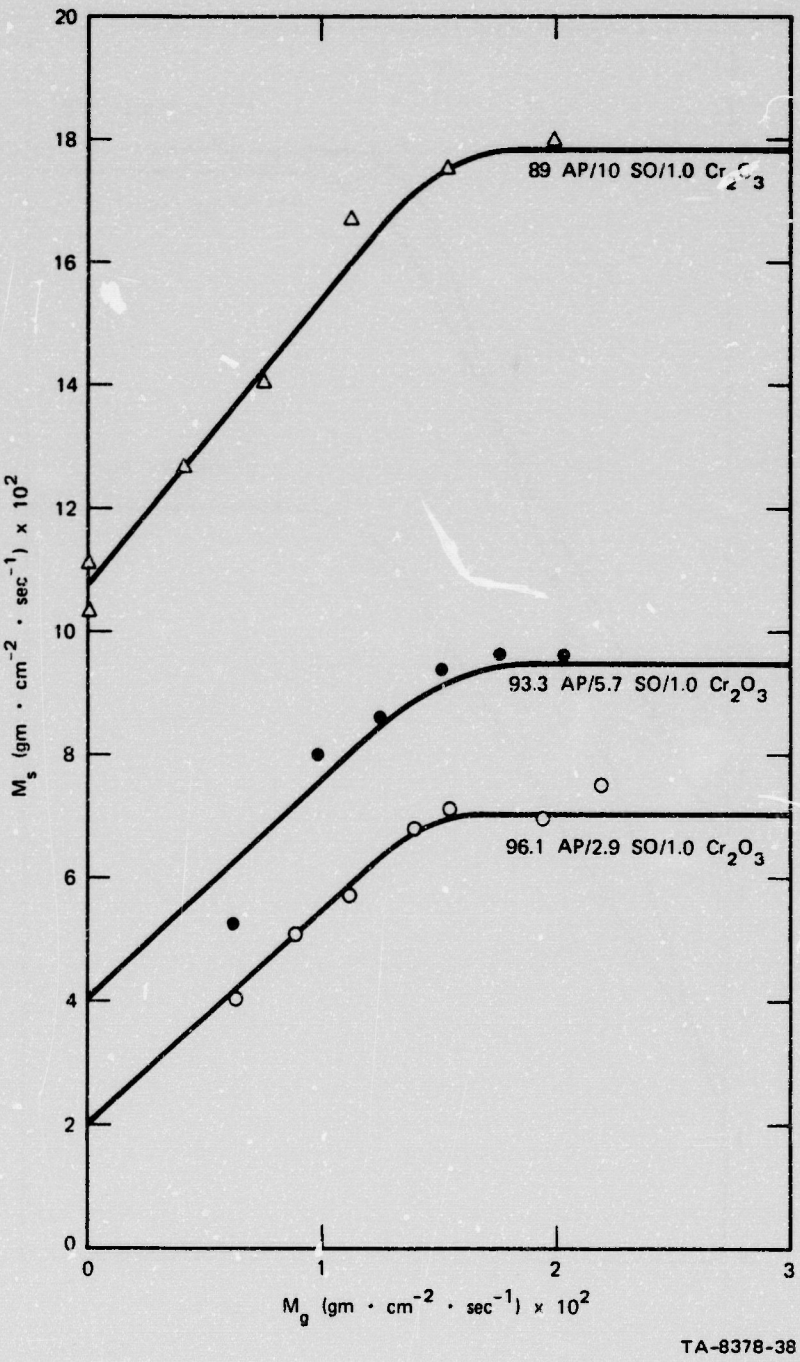

FIGURE 10 CONTRIBUTION OF SOLID FUEL AND CATALYST ON BURNING CHARACTERISTICS OF HOFD (SO = SUCROSE OCTAACETATE, CATALYST = Cr_2O_3; GAS = 24 VOL% C_3H_6)

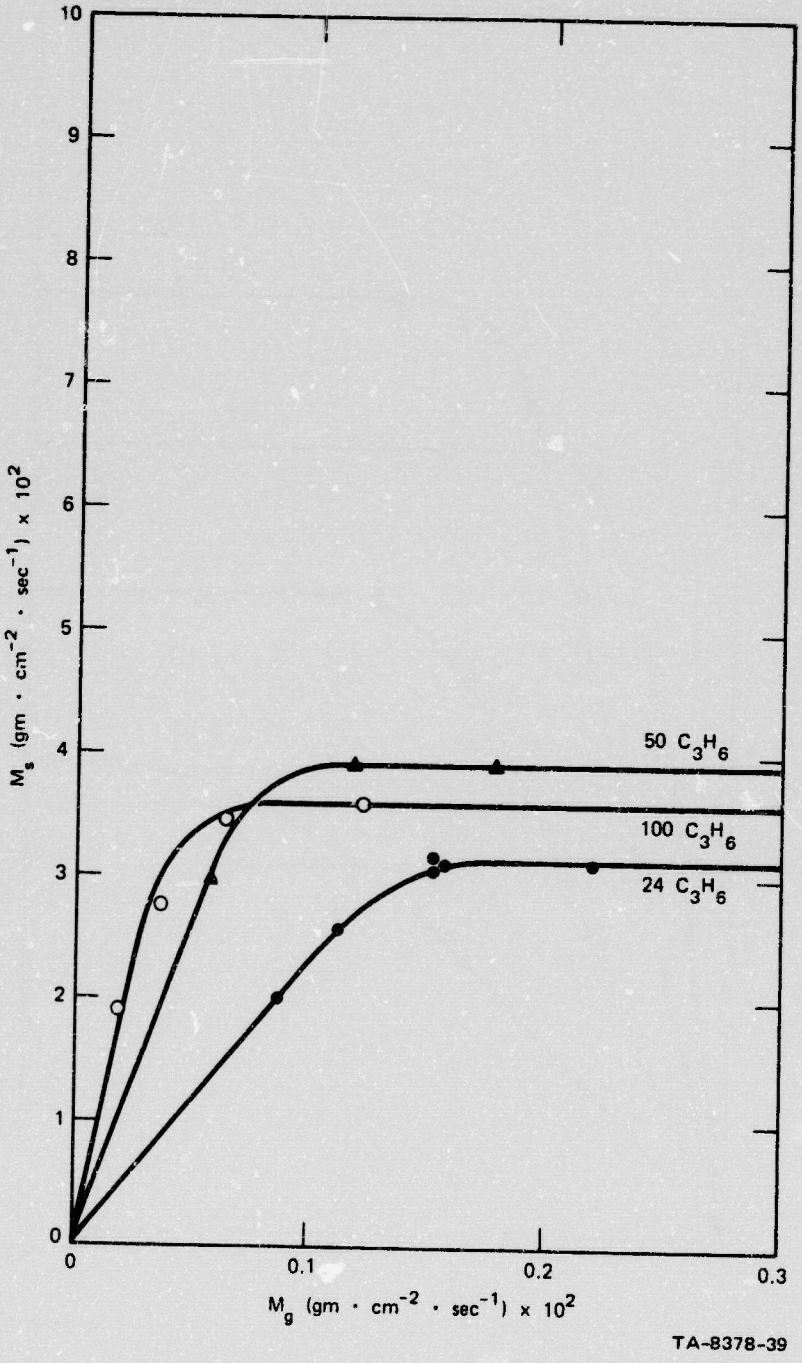

FIGURE 11 VARIATION OF AP MASS FLUX WITH GASEOUS FUEL MASS FLUX (SOLID: AP; FUEL: C_3H_6)

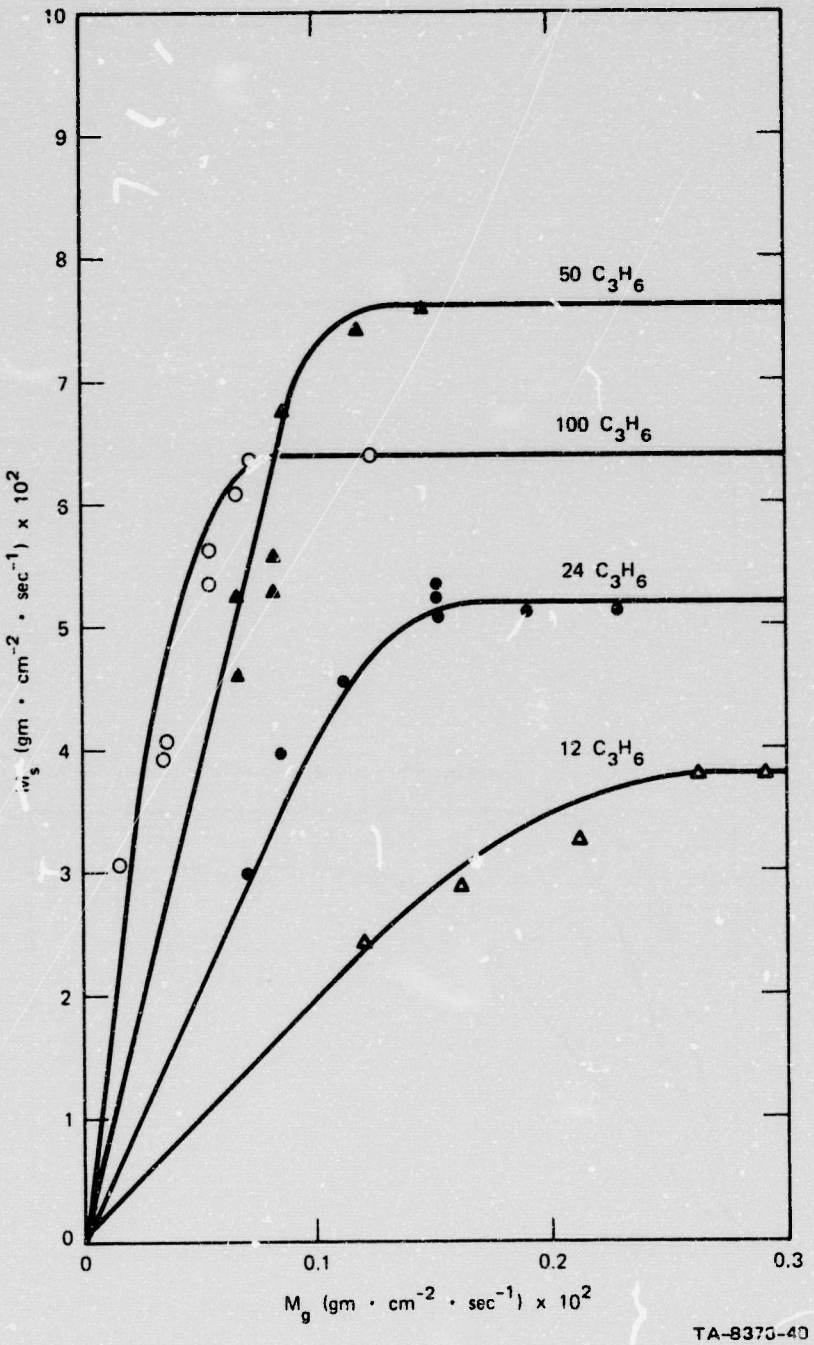

FIGURE 12 VARIATION OF SOLID MASS FLUX WITH GASEOUS FUEL CONCENTRATION (SOLID: 97.1 AP/2.9 CC)

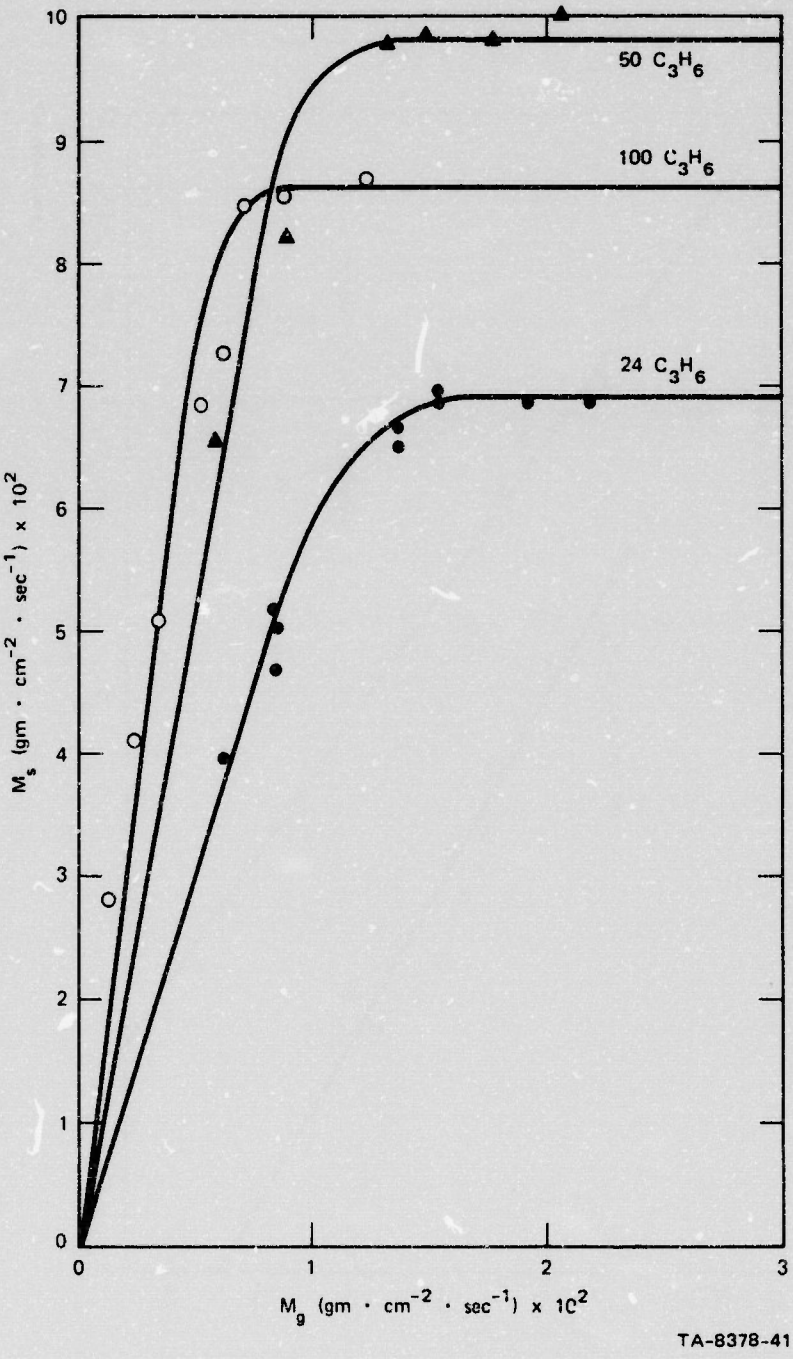

FIGURE 13 VARIATION OF SOLID MASS FLUX WITH GASEOUS FUEL CONCENTRATION (SOLID 95.2 AP/4.8 CC)

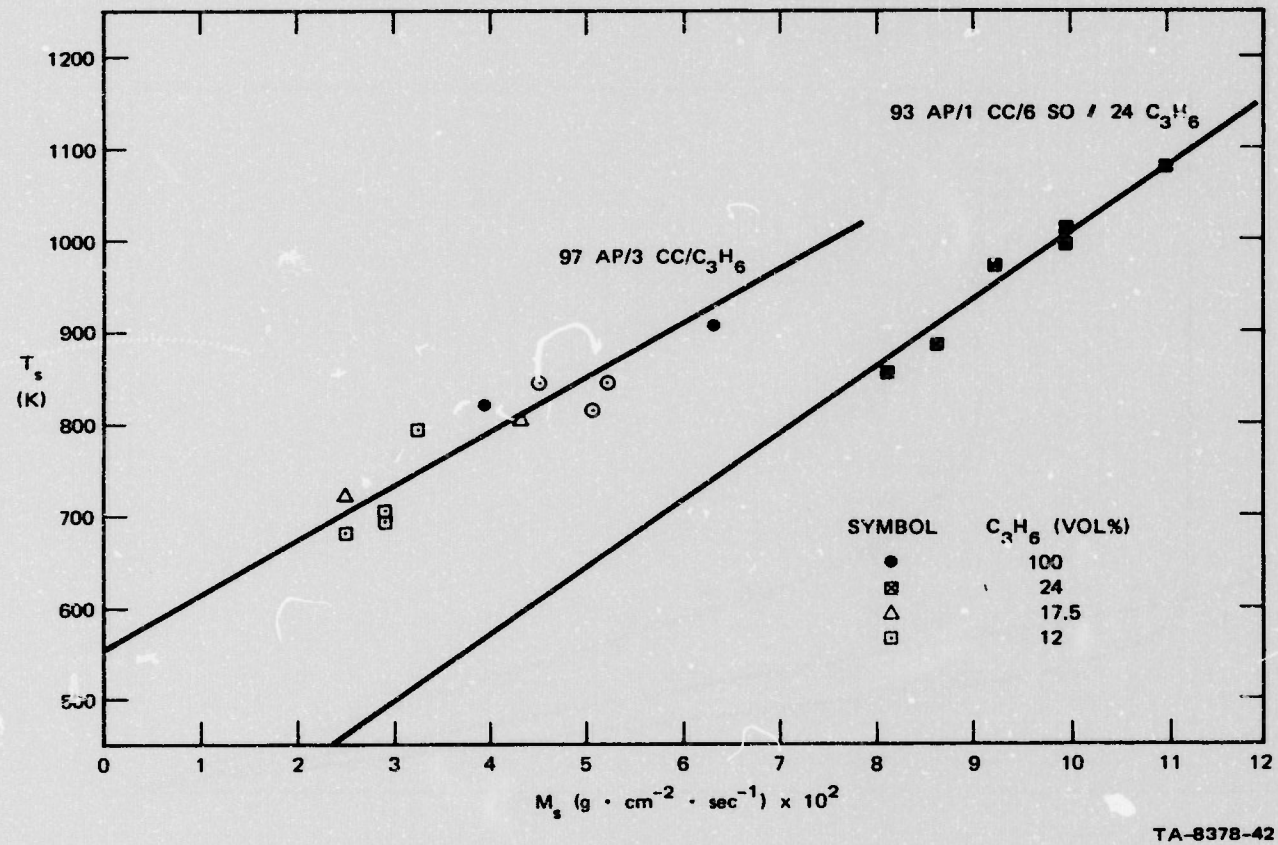

FIGURE 14 PROPELLANT SURFACE TEMPERATURES AT DIFFERENT REGRESSION RATES OF SOLID

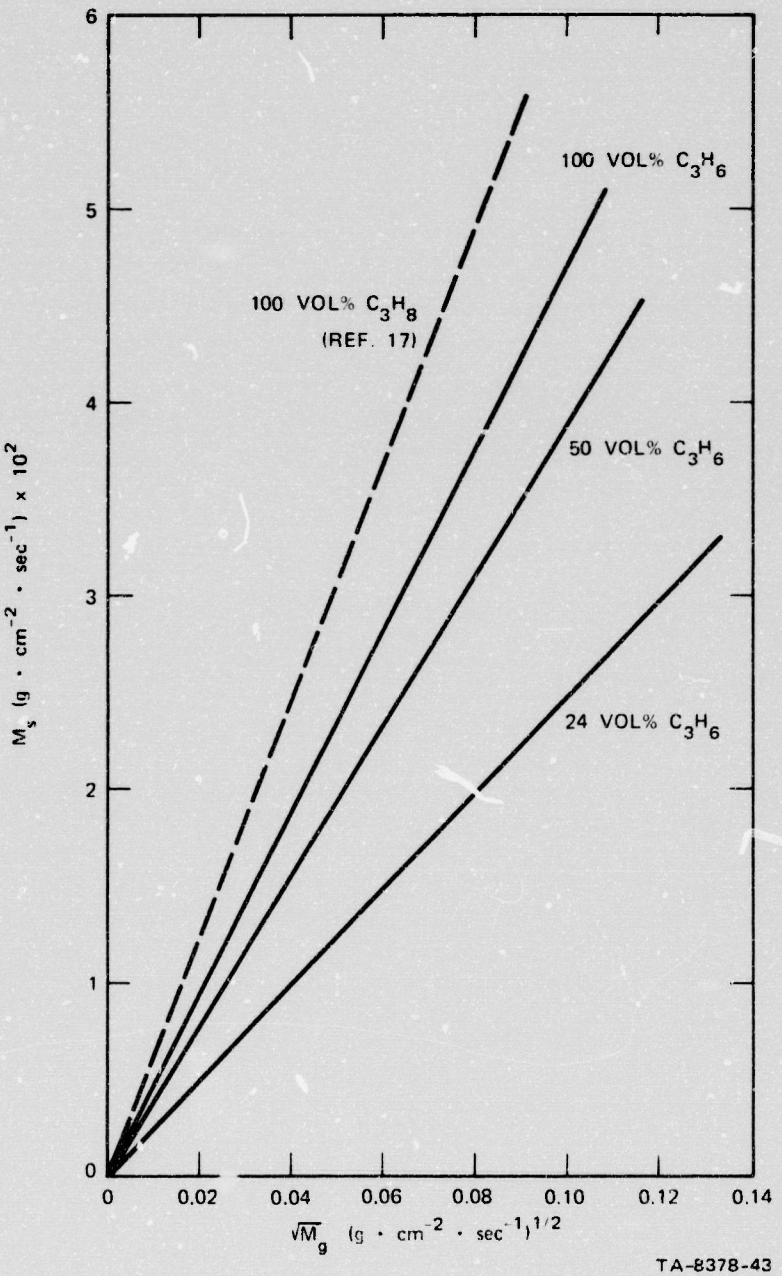

FIGURE 15 CORRELATION OF PROPELLANT MASS FLUX WITH FUEL MASS FLUX (SOLID PHASE: AP; FUEL: C_3H_6 OR C_3H_8)